

---

**APPLICATIONS OF HERMETICALLY SEALED FLUID DAMPERS  
FOR LOW LEVEL, WIDE BANDWIDTH VIBRATION ISOLATION**

---

by

**Alan R. Klembczyk, Chief Engineer**

**Taylor Devices, Inc.  
90 Taylor Drive  
North Tonawanda, NY 14120-0748**

and

**Michael W. Mosher, Shock and Vibration Analyst**

**Tayco Developments, Inc.  
90 Taylor Drive  
North Tonawanda, NY 14120-0748**

# **APPLICATIONS OF HERMETICALLY SEALED FLUID DAMPERS FOR LOW LEVEL, WIDE BANDWIDTH VIBRATION ISOLATION**

Alan R. Klembczyk, Chief Engineer  
Taylor Devices, Inc.  
North Tonawanda, NY 14120-0748  
716-694-0800

Michael W. Mosher, Shock and Vibration Analyst  
Tayco Developments, Inc.  
North Tonawanda, NY 14120-0748  
716-694-0800

Effective isolation systems for extremely low level, wide bandwidth vibration often require stringent performance properties throughout a wide range of operating conditions. A highly reliable and robust design necessitates simplicity, predictability, and repeatability. Analytical and empirical test results are presented from ongoing research that demonstrate the effectiveness of a relatively simple, yet highly effective passive isolation system, using a hermetically sealed fluid damper and mechanical spring combination to successfully isolate a given component from various vibration inputs.

## **INTRODUCTION**

Several techniques have historically been used to isolate the effects of vibration in sensitive components. These include the use of fluid dampers, elastomeric vibration isolators, tuned mass damper systems, and the optimization of a component's existing structural damping characteristics. While each of these methods have their own advantages, it is often difficult for the designer to provide the proper performance throughout the entire range of operating requirements and environmental extremes. For example, it is often necessary to eliminate static and dynamic seal friction (hysteresis) within the damping system while still allowing for no possibility of material leakage, out-gassing, or contamination of surrounding components. In addition to these requirements, the system might need to be completely passive with no power input, be designed for minimal weight, produce no magnetic fields and/or be consistent and reliable over environmental extremes.

Typical applications of isolators for low level, wide bandwidth vibration include high resolution cameras, optics, and sensitive structures for space-based vehicles. Many types of fluid filled isolators have been employed in these applications, and this type of device is the subject of this research report.

The properties of a frictionless fluid filled isolator are well matched to the demanding output criteria of the aforementioned applications. This is because a frictionless system is of prime importance when designing specifically for low level vibration isolation. Otherwise, the isolation system will simply act as a rigid mechanical link when subjected to low power spectral density (PSD) inputs and inevitably pass the unmitigated input directly to the payload, possibly amplifying the excitation to unacceptable levels. In addition, it is oftentimes impossible to analytically quantify this hysteretic effect in the frequency domain due to its nonlinearity. The maximum allowable friction value should be defined based on the level of vibration input such that the desired characteristics can then be designed into the system. The friction is also dependent on properties such as mass, stiffness, and effective viscous damping.

Figure 1 depicts a frictionless fluid isolator, where flexural metal bellows seals are employed, thus eliminating friction from sliding surfaces. The flexural metal bellows seals of the damper are accompanied by close clearance labyrinth seals for dynamic sealing of the damping fluid chambers. This arrangement ensures that the only hysteresis in the device is due to the friction of the sliding components on a small hydrodynamic film of oil. Labyrinth seals of this type operate essentially as a linear journal bearing, i.e. there is no intimate contact of any metal or elastomeric sliding components. In a zero G environment, the friction is reduced even further to that of the surface tension of the fluid itself. In either case, this level of friction can often be considered negligible, and this is verified by test results presented here.

A major concern of any type of sealed fluid system is leakage. To eliminate the possibility of leakage and therefore guarantee a completely hermetic system, the metal bellows flexural seal is attached and weld sealed to the piston rod and the cap of the damper. Since all joints are welded shut, there is no possibility of leakage or out-gassing. In order to assure no internal pressure build-up due to dynamic volume displacement, a crossover port is incorporated between each of the two metal bellows seals. This arrangement (U.S. Patent 4,638,895) is illustrated in Figure 1.

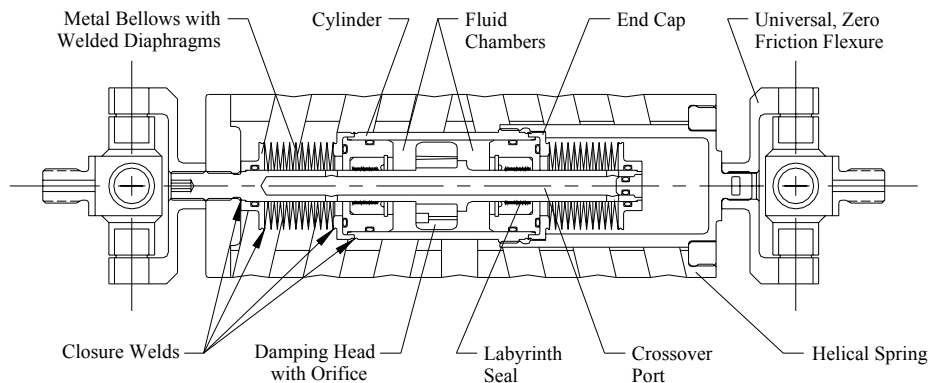


**Figure 1 Double Acting, Low Friction, Hermetically Sealed Vibration Isolator**

In order to maintain an acceptable and consistent output over a wide range of temperatures, different fluid flow techniques are often used. For example, a purely inertial fluid flow can be characterized by Bernoulli's Equation (1), which carries no dependence on fluid viscosity and therefore would be unaffected by temperature.

$$\frac{P_h}{\gamma} + \frac{V_h^2}{2g} + \frac{P_l}{\gamma} + \frac{V_l^2}{2g} \quad (1)$$

In Equation (1),  $\gamma$  is fluid density,  $g$  is the gravitational constant,  $P$  is pressure, and  $V$  is fluid velocity on the high and low pressure sides respectively. Simplifying this equation for the fluid damper of Figure 1 and solving for the differential pressure between fluid chambers yields:

$$\Delta P = \frac{\gamma V^2}{2g} \quad (2)$$

The inertial characteristics of fluid flow can then be coupled with the viscous effects of the fluid and very specific damping functions can be maintained. The advantage of this is that a linear system is approximated and analysis and predictability become less cumbersome.

Using this type of damper, it is possible to achieve virtually any amount of damping required. A very high level of damping (even over-critically damped) can be achieved since the damping system does not depend on an inherent stiffness property. At the same time, a desirable high frequency roll-off can be obtained by utilizing frequency dependent orificing combined with the inherent compressibility properties of the damping fluid. The level of the roll-off can also be increased using a fluid damper of this type since a truly linear system may not be able to provide enough roll-off at higher frequencies. This is especially true if the linear system is highly damped at resonance.

## **PROGRAM THEORY AND OBJECTIVES**

The isolation system for this research project had to be designed to meet a given transmissibility (TR) envelope over a broad range of random dynamic input presented in the form of a PSD defined between 1 and 500 Hz. The input ranged from a flat PSD level of  $8 \times 10^{-5} \text{ g}^2/\text{Hz}$  (.2 g rms) to  $2 \times 10^{-7} \text{ g}^2/\text{Hz}$  (.01 g rms) over the 500 Hz frequency band desired. It was necessary for the isolation system to remain fairly linear in response over the range of amplitudes that the system would be subjected to, i.e. the Transmissibility vs. Frequency needed to remain fairly consistent with varying PSD inputs.

For the purpose of analysis, it was desired that the system provide a peak TR of 2 at resonance, corresponding to a highly damped system. This equated to a damping level of 84% of critical for a similar linear system. A roll-off of -31 db/dec was then needed which is typical of a lighter damping level of 50% of critical for a similar linear system. Therefore, a linear system, as represented by a simple Kelvin model, cannot provide the performance required. The isolator of Figure 1 was designed to match the performance of a Maxwell model of a damper in parallel with a helical spring. This composite model is shown in Figure 2.

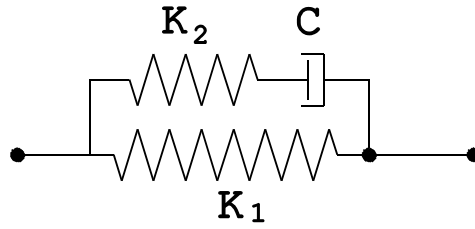


**Figure 2 Composite Model**

The model shown in Figure 2 can meet the high damping at low frequencies and low damping at higher frequencies required by the isolation envelope. This envelope is typical of many low input level isolation systems, especially those involving extremely sensitive payloads.

The TR is then formulated in terms of a transfer function as follows:

$$TR = \frac{C(K_1 + K_2)s + (K_1 K_2)}{(mCs^3) + (mK_2s^2) + (C(K_1 + K_2)s) + (K_1 K_2)} \quad (3)$$

where C is the damping constant,  $K_1$  and  $K_2$  are the respective spring rates of Figure 2, m is the isolated mass, and s is the LaPlace operand.

The result of this equation is represented by the ideal Transmissibility vs. Frequency plot, shown in Figure 3, which depicts an acceptance limit as well as a linear system that matches the peak of the design goal limit at resonance. It is evident that the idealized system offers a large performance benefit over the linear model.

The performance goal of this particular isolation system was to provide passive isolation in 5 rigid body degrees of freedom of the isolated mass, while not exceeding the TR acceptance limit. These included 2 translational and 3 rotational degrees of freedom, requiring a minimum of 5 isolators. Another requirement of the isolators was to remain essentially frictionless in all degrees of freedom, which includes motions both on and off the centerline axis of the individual isolators. If any appreciable friction was present, the mass would act as if the isolation system was rigid, and all the vibrational energy would be passed directly into it.

To provide the desired off-axis compliance, universal flexures were used at the isolator attach points. A frictionless universal flexure was used, made by combining three flexural pivots. Two were mounted in a single rotational axis, and the other was mounted in a second rotational axis. This arrangement is illustrated at both ends of the isolator of Figure 1.

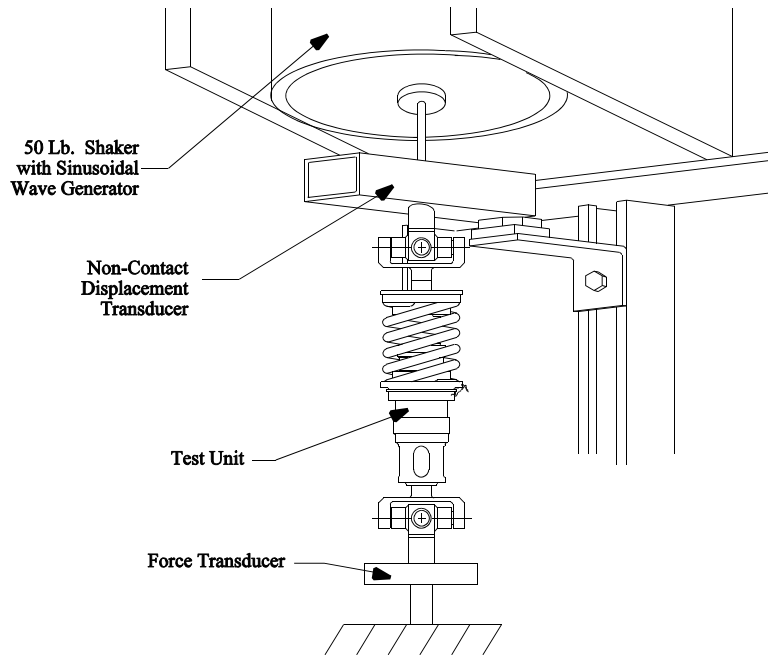


**Figure 3 Transmissibility vs. Frequency**

### **COMPONENT LEVEL TESTING**

In order to verify system performance, prototype isolators were fabricated and subjected to two phases of analysis and testing. The first phase was at the component level and the second phase was at the system level. Component level testing was performed on each isolator to determine individual output parameters. These results were used to determine the need for any adjustments before implementation into the actual system. From these component tests, an analysis was performed and a projected system transmissibility profile was generated. This profile was then verified later during system testing.

Component level tests generated an impedance transfer function relationship of Force/Velocity (F/V). This was used to determine the relationship of the damping coefficient of the isolator (over frequency) as compared to a linear system. The test set-up is shown in Figure 4. It consists of a 50 lb maximum force Unholtz-Dickie shaker connected to a non-contact displacement transducer which in turn is connected to the isolator. A force transducer is used to monitor isolator force. The input to the shaker is generated by a sinusoidal wave generator which sweeps through discrete frequencies from 1 to 500 Hz at a constant peak velocity. Linearity, which is defined as the change in the effective damping coefficient to the change in input velocity, was monitored from 1 to 30 Hz for different values of velocity over frequency.

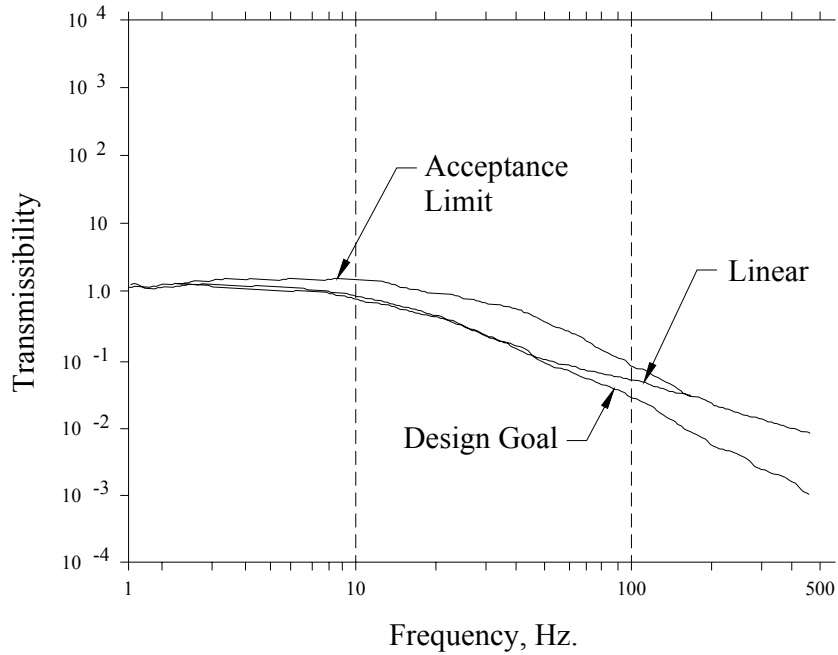


**Figure 4 Component Level Test Set-Up**

Based on the system analysis, the isolator was required to meet a specific transmissibility with respect to an equivalent dynamic mass. The actual component level test results were then fed back into the system analysis. The predicted system transmissibility is shown in Figure 5.

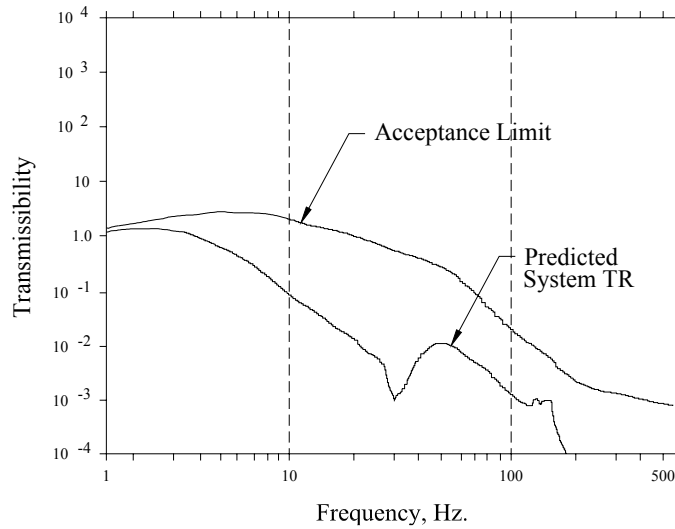


**Figure 5 Transmissibility vs. Frequency**

The predicted TR curve was generated through the use of the actual test data obtained during component testing on each of the five isolators used in the full-up system. Computer programs were written to account for the orientation of each isolator with respect to the center of gravity of the payload.

### SYSTEM TESTING

After completion of component tests and a post-test analysis of the results, a direct transmissibility test was performed to verify the predicted system transmissibility, as shown in Figure 5. System testing was again performed with each individual isolator supporting a representative mass. However, rather than a sinusoidal driving excitation, the input was a random excitation based on PSD levels of the actual operating environment. The acceleration was measured at the mass and was compared with the input PSD to determine the transmissibility.

The tests were first performed with an external spring mounted in a concentric fashion around the cylinder of the isolator. Testing at various PSD levels produced satisfactory results beginning at approximately  $8 \times 10^{-5} \text{ g}^2/\text{Hz}$  (.2 g rms). However, the isolator performance deteriorated as the input levels decreased to a point where unacceptable hysteretic behavior of the isolator was evident. This began to occur near a PSD of  $3 \times 10^{-6} \text{ g}^2/\text{Hz}$  (.04 g rms) and is evident in Figure 6. Note the unacceptable amplification at two resonant peaks. The source of friction in this case was found to be a small bending moment on the piston of the isolator which was being induced by a moment from the ends of the helically wound coil spring.

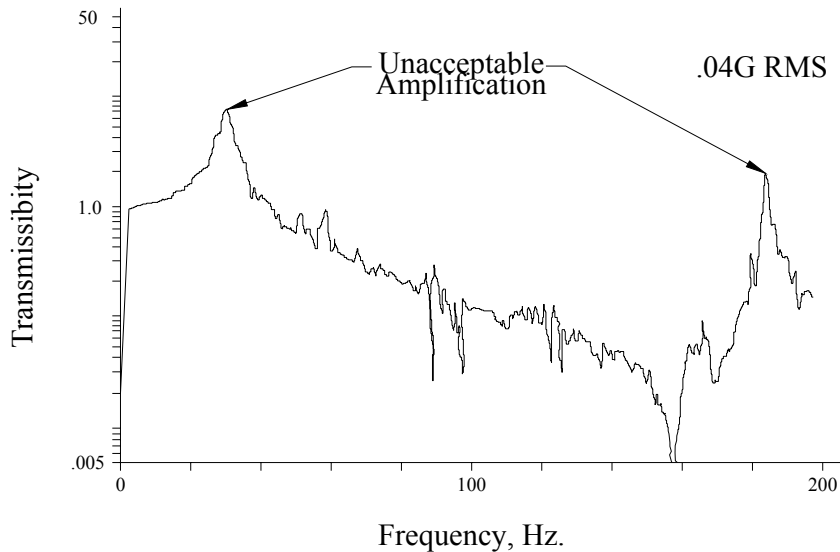


**Figure 6 Test Results: Isolator with Integral Coil Spring**



For the next series of tests, the helically wound coil spring was decoupled from the isolator and mounted in parallel. With this arrangement, the measured friction dropped to near zero. The transmissibility test now showed the desired performance at all levels of PSD input. Figure 7 shows the resulting transmissibility at an input of  $3 \times 10^{-6} \text{ g}^2/\text{Hz}$  (.04 g rms). Comparison of Figures 6 and 7 demonstrate the much improved performance after a simple reduction in isolator friction.

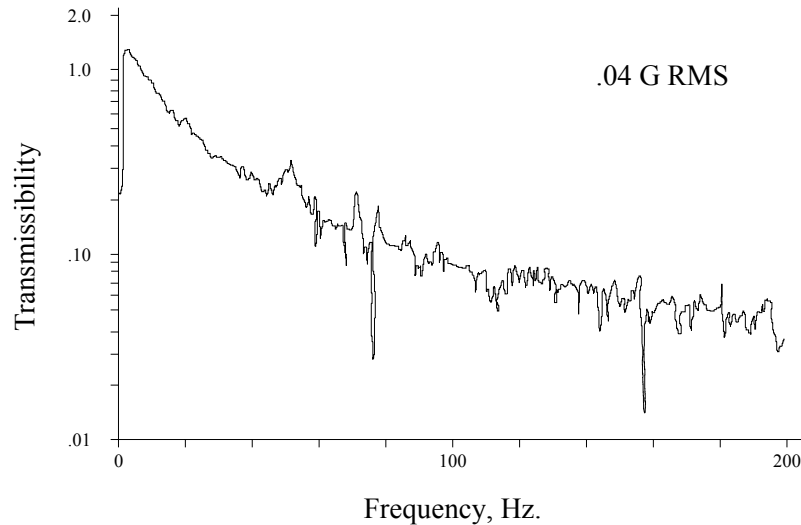


**Figure 7 Test Results: Isolator with Non-Integral Coil Spring**

The system tests demonstrated that the maximum amount of friction allowable in the isolators before the performance envelope was exceeded was approximately 3% of the maximum dynamic output force of the isolator, including both spring and damping force, when subjected to the lowest specified PSD level. In this particular case, the lower limit was  $2 \times 10^{-7} \text{ g}^2/\text{Hz}$  (.01 g rms).

Analytical efforts were then initiated in order to define an upper acceptance limit on isolator hysteresis for general use. Since the introduction of friction creates a non-linear system which is not easily adaptable to frequency domain techniques, a different approach was needed. This alternate approach was to generate a time domain realization of the lowest level PSD which was used as the input to a model of the isolator supporting the effective weight. This was done to derive the time domain response of the test mass. The resulting output signal was windowed and a Fourier transform generated to obtain the frequency domain representation. This was then compared to the input to generate the frequency response function representing the transmissibility of the isolator while supporting the effective weight. Friction of the model was increased until the performance envelope was exceeded. An example is shown in Figures 8 and 9 for a .01 g rms flat PSD spectrum from 1 to 500 Hz. Figure 8 shows the response of the isolator-mass model with zero friction. The response lies, as would be expected, along the idealized transmissibility curve. Figure 9 shows the response of the isolator-mass model with just .05 lbs. of friction introduced into the system. The deterioration in performance, especially at high frequencies, is quite evident.

The level of friction which can be considered to be allowable is specific to each application. However, results presented here indicate a good initial value that can be used for design purposes. The isolator design can then be altered during system testing if necessary. Ongoing research and data collection is presently being performed.

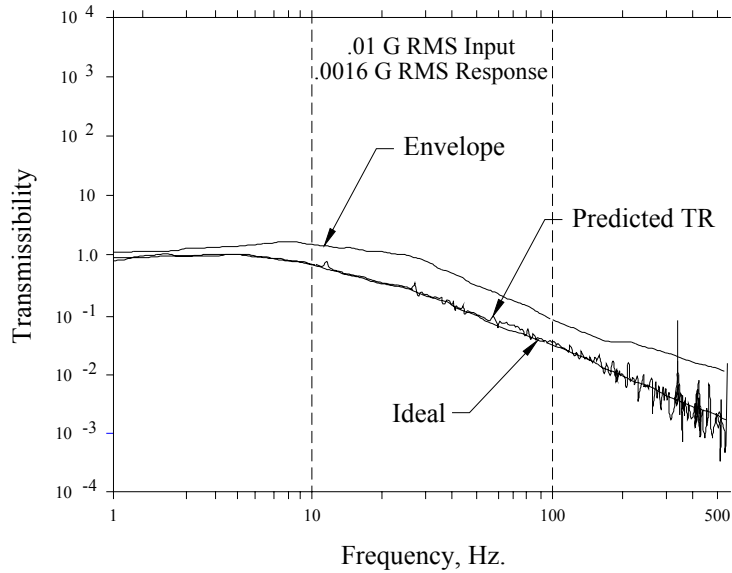


**Figure 8 Results of Analysis: Isolator with Zero Friction**

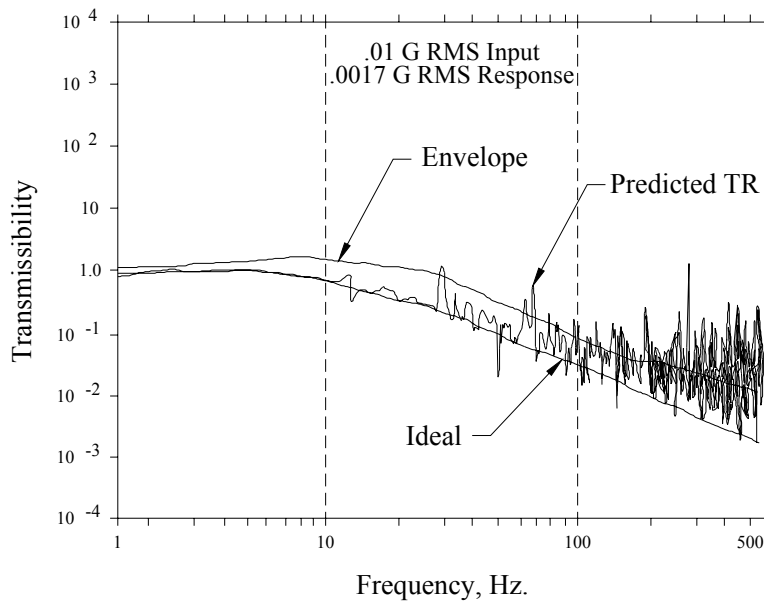


**Figure 9 Results of Analysis: Isolator with .05 lbs. Friction**

## CONCLUSIONS

Test results have been presented that validate the use of a relatively simple, robust, and predictable fluid filled isolator to mitigate the effects of low level, wide bandwidth vibration. This type of isolator has proven to be reliable for many extreme operating environments. Successful applications include high resolution camera isolators, flight control dampers, satellite solar panel deployment dampers, satellite gimbal over-travel shock absorbers, and gimbal vibration isolators for infrared seekers.

Verification of system performance can be achieved by performing the following procedure:

1. Define the random vibration input in terms of PSD and frequency bandwidth.
2. Develop a model of the isolator and generate a transfer function to determine preliminary damping output specifications.
3. Establish an upper limit for friction based on PSD input levels, bandwidth, and system parameters that satisfy a specified performance envelope. An acceptable level of friction found here was approximately 3% of the total isolator dynamic output force.
4. Perform component level testing to verify damping output and re-run the analysis to predict overall system performance.
5. Run a system test to define the transmissibility vs. frequency at various PSD inputs.

For the tests performed for this research project, the upper acceptance limit for isolator friction was demonstrated to be approximately 3% of the total isolator dynamic output force. This has also been verified by computer analysis for low level vibration isolators in the 500 Hz frequency range. This analytical technique is now available for future applications.

Ongoing research is presently being performed by the authors concerning the quantification of allowable isolator hysteresis. Additional information on this phenomena from others in the Shock and Vibration community would be appreciated.

## REFERENCES

- [1] Chen, Chi-Tsong, "Linear System Theory & Design," 1984, Oxford University Press, New York.
- [2] Soong, T.T., Grigoriu, Mircea, "Random Vibration of Mechanical & Structural Systems," 1993, PTR Prentice-Hall, Inc., Englewood Cliffs, New Jersey.
- [3] Thompson, William T., "Theory of Vibration With Applications," 3<sup>rd</sup> Edition, 1988, Prentice Hall, Englewood Cliffs, New Jersey.
- [4] Fitz-Coy, N, Chatterjee, A., "Actuator Placement in Multi-Degrees-of-Freedom Vibration Simulators," Proceedings of the 63<sup>rd</sup> Shock & Vibration Symposium, Vol. II, 1992.
- [5] Cunningham, David C., "Performance / Sizing Tradeoffs in Active & Passive Launch Isolation," Proceedings of the 63<sup>rd</sup> Shock & Vibration Symposium, Vol. I, 1992.